DEPARTMENT OF

NAVAL ARCHITECTURE & OFFSHORE ENGINEERING

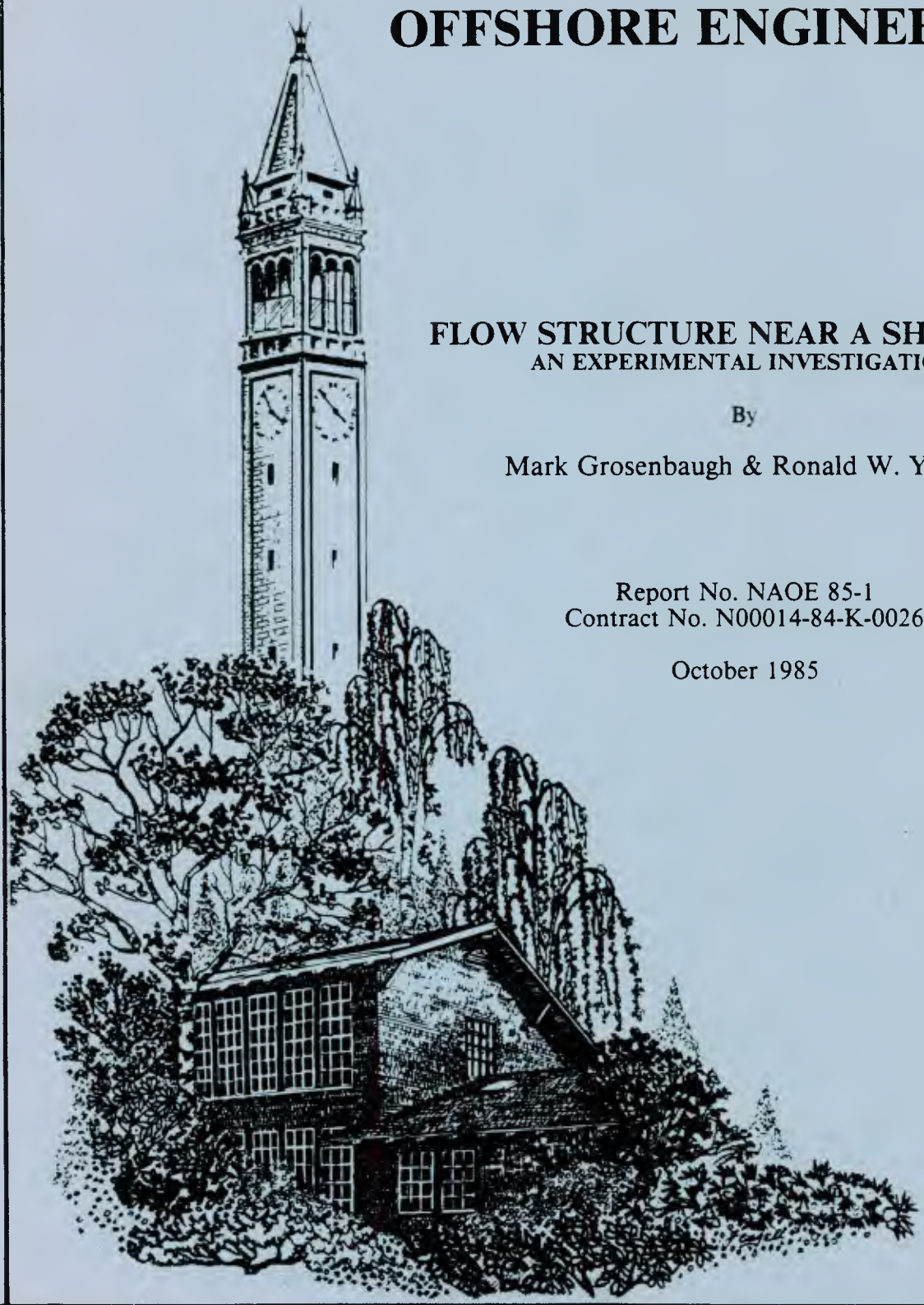

FLOW STRUCTURE NEAR A SHIP BOW:
AN EXPERIMENTAL INVESTIGATION

By

Mark Grosenbaugh & Ronald W. Yeung

Report No. NAOE 85-1
Contract No. N00014-84-K-0026

October 1985

UNIVERSITY OF CALIFORNIA, BERKELEY, CA 94720

(415) 642-5464

FLOW STRUCTURE NEAR A SHIP BOW:
AN EXPERIMENTAL INVESTIGATION

By

Mark Grosenbaugh & Ronald W. Yeung

Department of Naval Architecture & Offshore Engineering
University of California, Berkeley

Report No. NAOE 85-1

Supported by the
Office of Naval Research
under
Contract No. N00014-84-K-0026

October 1985

Abstract

Two dimensional flow near a ship bow is experimentally investigated by studying the flow around a horizontal, circular cylinder. The cylinder is held fixed in a flume. It is half submerged and extends from side to side so that all the flow has to go beneath it.

A bore-like structure develops at the bow of a cylinder when it is immersed in a current. Our observations indicate that the leading edge of this bow wave coincides with a point at which the main flow separates from the free surface. We show, experimentally, that the location of the separation point and the free-surface slope at the separation point are functions of the ratio Weber number / Reynolds number .

Systematic measurements reveal the existence of a well defined critical flow velocity at which the appearance of the free surface undergoes a transition from quiescent to turbulent. The critical velocities for two different sized circular cylinders, one of radius 2.54 centimeters and the other of radius 4.45 centimeters, are measured. The smaller cylinder has a critical velocity of 50 cm/s and the larger cylinder has a value of 52 cm/s. The near equality shows that the Reynolds number scaling for the critical velocity depends on a length scale associated with the cylinder's bow wave rather than the radius of the cylinder.

At flow velocities above the critical value, the bow waves are observed to oscillate at a characteristic frequency. This frequency, when nondimensionalized with the square root of the draft and gravitational acceleration, is a function of a draft Froude number that is based on the difference between the flow velocity and the critical velocity.

Table of Contents

List of Figures

1. Introduction

Presented in this report are the results of an experiment on flow past a two dimensional, horizontal cylinder. The cylinder was held fixed in a flume, was half submerged, and extended from side to side so that all the flow had to go beneath it. The intent was to simulate the flow at the bow of a two dimensional ship.

Mori (1984) used vertical cylinders to study the formation of the bow wave of a ship. He observed that, at a certain velocity, turbulent flow appears on the free surface near the bow. Above this velocity, the turbulent motion intensifies, and a breaking wave develops.

In the present experiment, we also observed that there was a *critical velocity* at which the free surface of the bow wave became turbulent.† Figure 1 shows the change in the form of the bow wave of a horizontal cylinder as the velocity passes through the critical value. Below the critical value (figure 1a), the surface of the bow wave, between the cylinder and the wave front, is smooth. As the velocity is increased (figure 1b), the surface becomes disturbed, and the capillary waves are fractured by longitudinal lines that extend out from the wave front. A further increase in the flow velocity (figure 1c) produces the fully turbulent appearance that Mori calls *sub-breaking*.

Above the critical velocity, the observed behavior of the bow wave of a horizontal cylinder was different from what Mori reports for the vertical case. Mori observes that the appearance of the bow wave is steady except for random fluctuations due to the turbulence. We found for the case of horizontal cylinders that, as the velocity is increased above the critical value, the form of the bow wave becomes unsteady. A prominent, oscillatory motion develops in the longitudinal position of the wave front and in the height of the free surface near the cylinder's bow. A comparison of figures 1d and 1e illustrates this phenomenon. The pictures were taken at different times but at the same flow velocity. Figure 1d shows the

† Mori found that the Reynolds number corresponding to the appearance of turbulence at the bow of a vertical cylinder was approximately 2.0×10^5 (based on the cylinder's radius of 21 centimeters). Our experiments were performed using horizontal cylinders, and we found that the Reynolds numbers for two different sized cylinders, one with radius = 2.54 cm and the other with radius 4.45 cm, were 1.1×10^4 and 2.0×10^4 respectively.

wave front close to the cylinder and the free surface elevated; figure 1e shows the wave front when its distance from the bow is a maximum, and the free surface, near the cylinder, is depressed.

In order to understand the phenomenon associated with the oscillation of the bow wave, it is important to understand why the bow wave exists. Patel et al. (1984) show, theoretically, that the presence of the bow-wave structure for a semisubmerged, two dimensional body is due to the presence of an upstream, stagnation point. He hypothesizes that, since there is an upstream point on the free surface at which the tangential velocity is zero, the incident stream must separate from the free surface, ahead of the body. Figure 2 shows a stream of dye incident on a two dimensional, rectangular body (the flow is from right to left). The stream of dye approaches the body and explodes into a *wake-like* structure. The dye is entrained into a wedge of fluid at the bow of the model. The main flow goes under this wedge and around the body. The separation point, defined as the point where dye is first entrained, coincides exactly with the wave front of the bow wave (for example, see figure 1). Patel et al. find that the separation point occurs where the free surface, rising up towards the body, achieves a slope equal to a specific value which depends on the Reynolds and Weber numbers. They use a double-body approximation to work out a formula for the location of the separation point for a circular cylinder. One of the objectives of this experiment was to test their hypothesis. We were able to measure both the location of the separation point and the slope of the free surface at the separation point for a circular cylinder. Previous experimental data by Kayo et al. (1982), Honji (1976), and Suzuki (1975) is contradictory. We will show that the results are sensitive to the amount of surface contaminates that are present on the water.

Another objective of the study was to analyze the oscillation of the bow wave. After the start of our work in 1983, some qualitative notions related to the possibility of bow-wave oscillation were mentioned by Miyata et al. (1984). Also, Miyata et al. (1985) obtained numerical results that indicate the existence of periodic motion of a two dimensional bow

wave. Still, there exists no systematic study of the phenomenon. In this report, are detailed measurements of the frequency and amplitude of the bow-wave oscillation as a function of velocity and model draft. An explanation is offered for the sudden onset of the oscillation that is seen in figure 1.

2. Experimental Procedure

The experiments were carried out in a circulating water channel (flume) that was 18 meters long and 61 centimeters wide. A water depth of 20 centimeters was used throughout the experiments. The maximum flow velocity achieved in this configuration, measured at the cylinder's location, was slightly over 95 cm/s.

Two dimensional, surface piercing flow was simulated by placing a half submerged, circular cylinder across the width of the flume (figure 3). The ends of the cylinder were flush against the walls of the channel for the initial tests. We found that, when the flow velocity fell below the critical value (defined as the velocity at which the appearance of the free surface near the bow went from calm to turbulent), the disappearance of turbulent motion allowed surface contaminates to collect in front of the cylinder. This affected the characteristics of the bow flow. Consequently, some of the tests were run on cylinders that had 5 millimeter gaps between their ends and the walls of the flume. This allowed the layer of surface contaminates to drain around the ends. Throughout the rest of this report, the two end configurations will be called *blocked* and *unblocked*. Two different size cylinders were used during the experiments. The light colored one shown in figure 3 is 5.08 centimeters in diameter and the dark colored one pictured in figure 1 is 8.89 centimeters in diameter. Another geometry, a rectangular cylinder with a faired underbody, was tested. The results will be presented in a future report.

Flow velocity was measured with a Marsh-McBirney, model 201, flow meter that was mounted underwater, downstream of the cylinder. The flow velocity at the cylinder was calibrated with the downstream velocity to take into account any variations along the length of the flume.

Our fixed model approach made observations and data collection easier than would have been possible in a tow tank. The drawback with using the flume was that disturbances to the flow field, produced by the pump, threatened to effect the measurements. We were able to damp out much of the fluctuations in the flume's water level by placing Honeycomb flow

straighteners upstream of the model. The effect of the remaining disturbance, associated with long period seiching in the channel, was minimized by letting the global flow reach a steady state before taking any measurements.

The slope of the free surface at the separation point was determined from bow-wave profiles of the 5.08 centimeter cylinder.† The profiles were measured with a resistance wave gauge mounted on a moving carriage. An experimental run consisted of placing the carriage upstream and moving it towards the cylinder at a rate equal to the flow velocity. A mechanical stop prevented the carriage from running into the cylinder. The analog signal produced by the wave gauge was amplified by a carrier amplifier, converted to a digital output, and recorded for every 2 millimeters that the carriage moved. The location of the carriage was measured with a linear position transducer that consisted of a cable, one end attached to the carriage, the other end wrapped around a spring-loaded potentiometer. This experimental technique worked well for flow velocities above 50 centimeters per second. Below that value, the changes in the water level of the flume made it difficult to measure the true slope.

The location of the separation point coincides with the wave front of the bow wave. Its position, relative to the cylinder, was measured by using a wire probe as a marker. For flow velocities above the critical value, where the wave front oscillated back and forth, the maximum and minimum positions were measured and then averaged.

The oscillatory motion of the bow wave was studied by placing a wave gauge at the bow of the cylinder and measuring the free-surface elevation as a function of time. The resulting signal, after being amplified and converted to digital output, was sampled at 25 samples per second for 40 seconds. The mean free-surface elevation, the standard deviation, and the spectral density were then computed from the time records. A second wave gauge was placed upstream to monitor the water level fluctuations in the flume.

† Bow wave profiles for the larger cylinder were not recorded.

3. Results

3.1 Separation Point

Figure 4 shows one of the instantaneous wave profiles that was used to study the slope at the separation point. The separation point was identified on all the records by looking for where the monotonically rising free surface encountered a discontinuity in its slope. The slope of the free surface, just before the separation point, was then measured from the profile plots. Profiles were recorded at flow velocities between 50 and 90 cm/s. For each velocity, five records were taken. A series of experimental runs was also made using water whose surface tension had been lowered by the addition of surfactant (Neodol® 25-7). Surface tension of water specimens was determined by measuring the height to which water was drawn up a capillary tube.

The values of the slopes are plotted versus the *separation number* (separation number = Weber number / Reynolds number) in figure 5. The solid curve represents the theoretical prediction of Patel et al. (1984). His equation for the free-surface slope at the separation point is

$$slope = \tan\left[\frac{2 \times Weber\ no.}{Reynolds\ no.}\right] \tag{1}$$

The bars correspond to the range of free-surface slopes measured for a particular *separation number* (separation number = Weber number / Reynolds number). Each symbol represents the average of the maximum and minimum slope values.

Figure 6 is a plot of the distance that the separation point was from the bow (nondimensionalized with the cylinder's radius) versus the draft Froude number (draft = cylinder radius). For higher velocities, where the bow wave oscillated, the minimum and maximum positions were measured and are plotted using a bar to represent the range for a particular Froude number. The solid curve is the solution of the equation derived by Patel et al. (1984) for the location of the separation point. The equation is

$$\frac{4F_d^2\left[(1+\beta)^2-1\right]}{\left\{(1+\beta)^{10}+16F_d^4\left[(1+\beta)^2-1\right]^2\right\}^{1/2}+(1+\beta)^5}=\tan\left(\frac{2\times Weber\ no.}{Reynolds\ no.}\right) \qquad (2)$$

where F_d is the draft Froude number and β is the separation distance divided by the cylinder's radius.

The separation point locations for both cylinders were measured with the ends unblocked. Figure 7 shows what occurs as a result of blocking the ends. At velocities below the critical value, dust and surface film collect between the separation point (identified by injecting dye into the flow) and the capillary waves. As the flow velocity decreases, the stagnant zone gets larger, and the capillary waves move away from the body. If the location of the capillary waves is erroneously taken as the separation point, results similar to those reported by Kayo et al. (1982) would be obtained. The presence of the stagnant boundary layer acts like a plate and causes the boundary layer to separate farther upstream than it normally would in the absence of surface contamination. This could explain why the experimental results of Honji (1976), for the separation point of a cylinder, would lie above the theoretical curve when plotted in figure 6 even though the radius of his cylinder (radius = 5.00 cm) was close to that of the larger cylinder of the present experiment. Our results are most similar to Suzuki's (1975) even though our cylinders were much smaller than those used by him (Suzuki's cylinders had radiuses of 10.7 cm and 13.5 cm respectively).

3.2 Oscillating Bow Flow

The critical velocity is qualitatively defined as the velocity at which the free surface undergoes a transition from a calm appearance to a turbulent one. We determined the value, quantitatively, by plotting the standard deviation of the bow-wave record versus the velocity (see figure 8). The crosses in figure 8 are the standard deviations of the upstream wave gauge and are a measure of the noise in the flume. Two trends in the data stand out. At low velocities, the standard deviations of the bow-wave records are small and nearly constant. At higher velocities, the values increase linearly away from the noise level and continue to get

larger with increases in the flow rate. The critical velocity is taken at the intersection of these trends. The value is almost the same for both cylinders, 50 cm/s for the smaller cylinder and 52 cm/s for the larger cylinder.

Beginning with the critical value, the time records for the bow wave gauge were fast Fourier transformed. Periodograms were calculated from the raw spectra and smoothed with a bandwidth of 0.05 Hertz. The resulting estimates of the spectral densities for the 5.08 centimeter cylinder are given in figure 9 and those for the 8.89 centimeter cylinder are given in figure 10. The peak frequency for the smaller cylinder increases from 1.2 Hertz measured just above the critical velocity to 1.4 Hertz corresponding to the highest recorded velocity. For the larger cylinder, the peak frequencies increase with velocity from 0.95 Hertz to 1.2 Hertz. Figure 11 shows a plot of the peak frequency (nondimensionalized with the draft and gravitational acceleration). The $X-axis$ is the reduced Froude number which is defined as

$$Reduced\ Froude\ No. = \frac{V - V_{crit}}{\sqrt{g \times draft}} \tag{3}$$

where g is the gravitational acceleration.

The mean of the time records for the wave elevation just in front of the bow was nondimensionalized by the total head of the incident flow and plotted versus the reduced Froude number (see figure 12). The total head represents the increase in the height of the free surface that would be expected if all the kinetic energy was transformed into potential energy. Thus, the maximum value to be expected is 1.0.

Blocking the ends of the cylinder has an interesting affect on the bow-wave oscillation. As the flow rate is lowered to near the critical velocity, surface contaminates collect at the bow of the cylinder. This is because there is less mixing due to the disappearance of turbulent motion on the free surface, and the blocked ends prevent the surface film from draining around the sides. As the velocity is slowly lowered and the amount of contaminates increase, the bow-wave oscillation reappears but at a higher frequency than before. As the flow velocity is decreased, the strength of the oscillation reaches a maximum and then dies

out, disappearing for all subsequent reductions in flow rate. We call this high frequency oscillation, which occurs below the critical velocity, *subcritical oscillation.*

Figure 13 shows the spectral densities for the 8.89 centimeter cylinder with the ends blocked. The oscillation seems to disappear at 58.4 cm/s. But the power spectrum for 51.5 cm/s shows the emergence of a higher frequency oscillation, which remains present in the spectral records down to approximately 45 cm/s. Above 58.4 cm/s, the power spectra for the blocked and unblocked cases (compare figures 10 and 13) are nearly the same.

We were able to induce a subcritical oscillation for the unblocked case by pouring surfactant, Neodol® 25-7, onto the water surface, upstream of the cylinder. When we did this, the surfactant was carried downstream and collected at the cylinder's bow. The capillary waves were pushed away from the cylinder and the bow wave assumed an appearance similar to that pictured in figure 7. If the flow rate was slightly below the critical velocity, then a subcritical oscillation would commence. This would proceed until the surfactant had drained around the unblocked ends leaving the wave front in its original position. If the flow velocity was too low then there would be no subcritical oscillation, just as in the blocked case.

Takekuma and Eggers (1984) report that the critical velocity for a ship model can be lowered by dragging a piece of vinyl on the water surface ahead of the model. They conclude that the presence of the vinyl sheet acts to increase the intensity of the free-surface shear layer. The above observations indicate that the layer of surface contaminates at the bow of the cylinders is performing the same function as the vinyl.

The 8.89 centimeter cylinder was also towed in the University of California Towing Tank to show that the oscillatory phenomena was not due to the natural mode of the flume. The results of these tests confirmed the existence of a well defined critical velocity, above which, the bow wave oscillated. We also observed a subcritical oscillation even though there was a large gap between the tow tank walls and the ends of the cylinder. (The tow tank is 2.64 meters wide; compare that to the cylinder width of 0.60 meters). The subcritical oscillation was triggered when dust and other contaminants, which were lying on the water surface

of the towing tank, became concentrated at the bow of the moving cylinder. This behavior is analogous to the unblocked case in the flume when large amounts of surfactants were poured onto the water surface upstream of the cylinder.

The frequency of the bow-wave oscillation in the towing tank was measured by timing ten cycles of the motion with a stopwatch. We also measured the oscillation frequencies in the flume using the same procedure. Figure 14 shows the plot of the oscillation frequency versus velocity (towing velocity for the towing tank data and flow velocity for the flume data). It is important to note that the cylinder ends were blocked for the flume measurements so that the subcritical oscillation frequencies could be compared. Also, notice the change of frequency at 100 cm/s for the tow tank data. This is where the bow-wave height became so large that part of the flow washed over the top of the cylinder.

4. Discussion

The measurements of the slope of the free surface at the separation point (figure 5) show that the trends, predicted by Patel et al. (1984), are correct. The slope is directly proportional to the flow velocity and inversely proportional to the surface tension. However, the actual values, as predicted by the theory, underestimate our experimental data. This may be due to the simplifying assumption made by Patel et al. that the surface tension is balanced by the viscous forces so that there would be no jump in pressure across the air-water interface.

The distance from the bow of the cylinder to the separation point is overestimated by the double-body model of Patel et al. (1984) as shown in figure 6. The double-body model is derived using the separation criteria theory. An underestimation of the value of the slope at the separation point produces an overestimation in the predicted location of the separation point (see equation 2). Thus, the discrepancies in the slope and separation location data with their respective theories are consistent.

The separated flow pictured in figure 2 appears to spread out from the separation point like a wake, entraining fluid from the main stream. If the wake were behind the body, it would continue to grow. Here the wake is upstream, and the presence of the body causes the fluid of the wake to converge into a boundary layer that travels around the bow.

The dynamics of the bow-wave oscillation appears to be a function of the mass and momentum flux into and out of this separated flow region. Below the critical velocity, any influx of fluid into the region is offset by an equal amount of fluid leaving the region so that a steady state is maintained. At the critical velocity there is an injection of fluid into the region, evidenced by the appearance of turbulent motion on the free surface. The excess fluid piles up at the bow to such a height that the free surface is unstable, and the excess water spills forward, pushing the wave front further ahead of itself. The wave front travels a short distance upstream before it is repulsed by the incident stream and driven back toward the bow of the cylinder. As the wave front is pushed back toward the body, much of the excess fluid is swept downstream in the main flow. The outflux of fluid abates, and there is a large

influx of new fluid. This causes the previously described motion to repeat itself.

As the flow velocity is increased above the critical value, the amplitude of the motion gets stronger (see figure 8), and the frequency of oscillation becomes higher (see figure 11). Figure 11 also shows that, if the frequency data is nondimensionalized with the square root of the draft and one over the square root of the gravitational acceleration, the curves produced by the two cylinders are approximately equal. This implies that the oscillation phenomenon is due to a sloshing-type oscillation rather than vortex shedding, which is described by a Strouhal number (in which case the oscillation frequency would be proportional to the draft and inversely proportional to the velocity).

Qualitatively, the increase in oscillation frequency can be attributed to more and more fluid entering the separated region and causing the free surface to reach an unstable height at a faster rate. There is still an outflux of fluid but its rate does not increase enough to maintain a balance with the influx. Hence, the equilibrium can only be restored by increasing the oscillation frequency. Consider figure 14. When the larger cylinder was towed in the towing tank, fluid flowed around the ends, and this increased the rate of outflux from the separated region. The effect was that the oscillation frequency was lower in the towing tank than in the flume for the same velocity. When the towing velocity reached 100 cm/s the free surface became high enough for the flow to go over the top of the model as well as around the ends. This increased the outflux rate even more and, as expected, figure 14 shows the oscillation frequency decreasing for velocities that are above 100 cm/s.

Mathematically, the oscillation can be thought of in terms of the complex eigenvalues associated with a certain linearized equation of motion. The eigenvalues are functions of the flow velocity. Below the critical value, the real part of all the eigenvalues is negative, and the behavior, associated with these solutions, decay with time. At the critical value, the real part of one of the eigenvalues becomes positive, and now the behavior associted with that solution will exist for large time. As the flow velocity increases, the real parts of other eigenvalues will become positive and affect the motion. Looking at the spectral densities for the larger

cylinder (figure 10), a new spectral peak, at a slightly higher frequency than the initial peak, begins to emerge at 80.3 cm/s and grows in strength as the flow velocity increases. The emergence of a second peak does not appear to occur over the measured range of velocities for the smaller cylinder.

Figure 12 shows that, below the critical Froude number, the mean amplitude, nondimensionalized with the stagnation height, is constant with respect to changes in the flow velocity. As the bow wave begins to oscillate, the mean amplitude decreases, eventually reaching a constant value. Notice that the nondimensional data for the two cylinders plot onto curves of similar shape but that the curves are displaced from each other. The fact that they do not collapse onto the same curve could be due to the presence of the shear layer that separates the main flow from the bow-wave region. Thus, it would be more appropriate to use a local velocity associated with the bow wave when calculating the stagnation height rather than the global flow velocity.

5. Conclusion

The present experiment confirms that the main flow separates from the free surface in front of two dimensional surface piercing bodies. The slope of the free surface at the separation point increases with separation number (Weber number / Reynolds number), and the values of the slopes are greater than those predicted by the simplified theory of Patel et al. (1984).

Our observations indicate there is a critical flow velocity at which the appearance of the bow wave of two dimensional, circular cylinders undergoes a transition from quiescent to turbulent. Above this critical velocity, the bow wave develops a periodic oscillation. The frequency of the motion scales nondimensionally according to gravity and the square root of the draft. It is also a function of a draft Froude number that is based on a velocity in excess of the critical value.

For the two cylinders used in this experiment, the critical velocities were 50 cm/s for the cylinder with a radius equal to 2.54 centimeters and 52 cm/s for the cylinder with a radius of 4.45 centimeters. The near equality in the values show that the Reynolds number scaling for the critical velocity depends on a length scale associated with the cylinder's bow wave rather than its radius.

The bow-wave oscillation appears to be due to a balance between the rate at which fluid is being entrained into the separated region and the rate at which it is exiting. As the net flux of fluid elevates the free surface, gravity and surface tension act as vertical restoring forces and cause excess fluid near the bow of the cylinder to spill forward. A horizontal restoring force due to the inertia of the main stream pushes the spilling wave front back toward the bow to begin a new cycle.

Acknowledgements

We would like to thank Professor R. A. Denton of the Department of Civil Engineering for the use of the Hydraulics Engineering Laboratory. We also wish to thank Lyn Magel for assisting with the electronics, and Bart Duncil for machining the experimental apparatus.

The authors gratefully acknowledge the Office of Naval Research for supporting this research under the Special Focus Program in Ship Hydrodynamics (Contract N00014-84-K-0026).

References

Honji, H., *Observation of a Vortex in Front of a Half-Submerged Circular Cylinder,* **J. Physical Society, Japan**, Vol. 40, No. 5, 1976.

Kayo, Y., Takekuma, K., Eggers, K., and Sharma, S.D., *Observations of Free-Surface Shear Flow and its Relation to Bow Wave-Breaking on Full Forms,* **Inst. Shiffbau, Univ. Hamburg, Report No. 420**, 1982.

Miyata, H., Kajitani, H., Matsukawa, C., Suzuki, N., Kanai, M., and Kuzumi, S., *Numerical and Experimental Analysis of Nonlinear Bow and Stern Waves of a Two-Dimensional Body (second report),* **J. Soc. Naval Arch. Japan**, No. 155, pp. 11-17, 1984.

Miyata, H., Kajitani, H., Shirai, M., Sato, T., Kuzumi, S., and Kanai, M., *Numerical and Experimental Analysis of Nonlinear Bow and Stern Waves of a Two-Dimensional Body (fourth report),* **J. Soc. Naval Arch. Japan**, No. 157, pp. 15-33, 1985.

Mori, K., *Necklace Vortex and Bow Wave Around Blunt Bodies,* **Proc. 15th ONR Symposium on Naval Hydrodynamics**, pp. 9-20, 1984.

Patel, V.C., Landweber, L., and Tang, C.J., *Free-Surface Boundary Layer and the Origin of Bow Vortices,* **Iowa Inst. of Hydraulic Res. Report, No. 262**, 1984.

Suzuki, K., *On the Drag of Two-Dimensional Bluff Bodies Semi-Submerged in a Surface Flow,* **Journal of The Society of Naval Architects of Japan**, Vol. 137, 1975.

Takekuma, K. and Eggers, K., *Effect of Bow Shape on Free-Surface Shear Flow,* **Proc. 15th ONR Symposium on Naval Hydrodynamics**, pp. 387-400, 1984.

Table 1

Summary of Critical Values		
	Cylinder #1	Cylinder #2
Radius	2.54 cm	4.45 cm
Critical Velocity	50 cm/s	52 cm/s
Critical Reynolds No.	11,100	20,300
Critical Froude No.	0.79	1.00

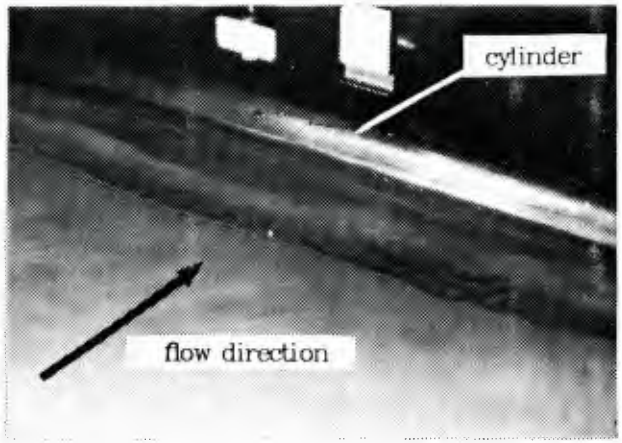

1a- Velocity ~50 cm/sec (just below critical; surface is calm).

1b- Velocity ~ 52 cm/sec (surface becomes disturbed).

1c- Velocity ~ 55 cm/sec (fully turbulent).

1d- Velocity ~58 cm/sec (wave front begins to oscillate).

1e- Same velocity as 1d; wave height is at maximum near the bow.

FIGURE 1: Series of photographs showing the change in the appearance of the bow wave as the flow velocity is increased through the critical velocity. The flow is from left to right.

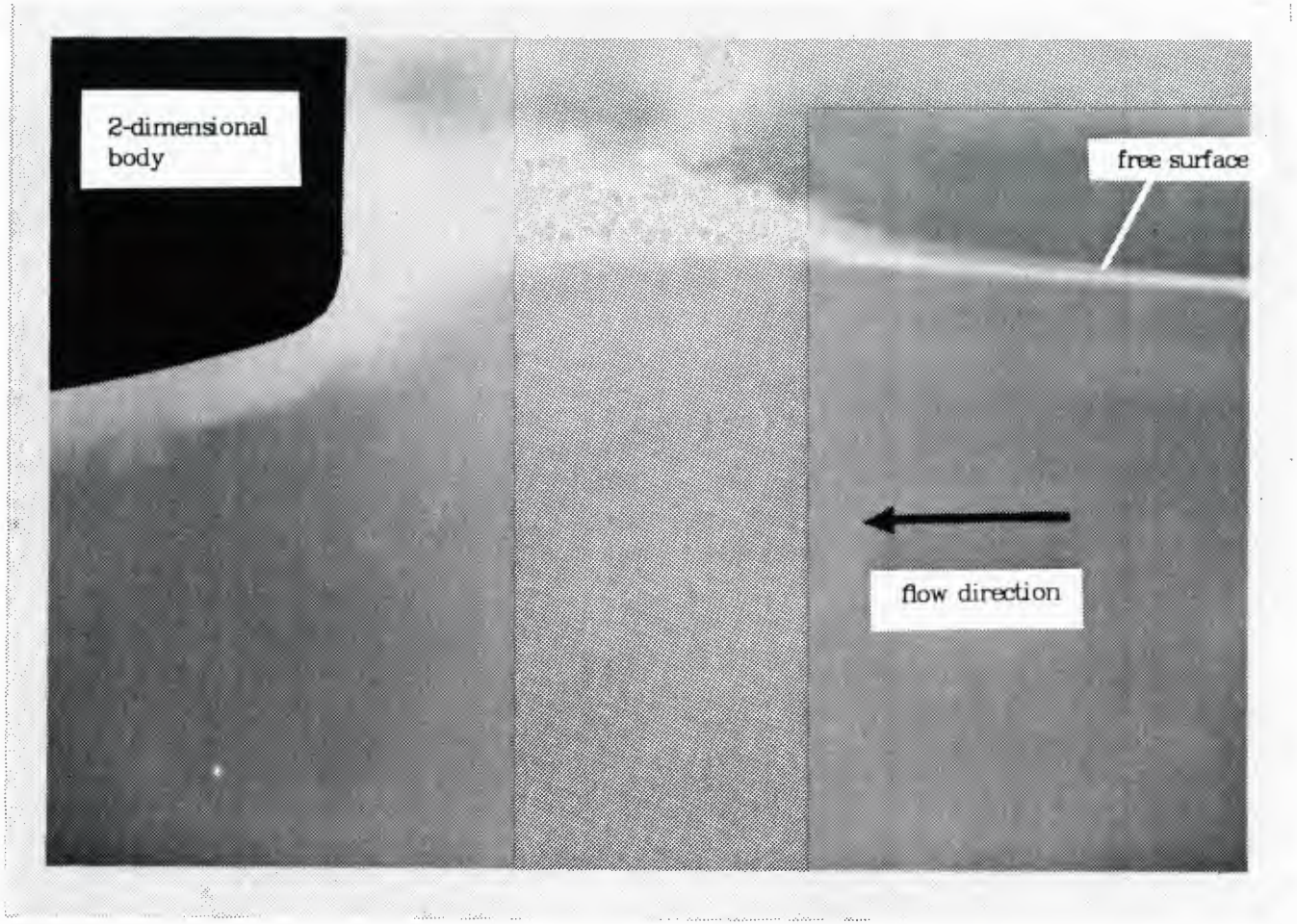

FIGURE 2: Flow visualization of the separation of the free surface streamline ahead of a rectangular cylinder. (Flow is from right to left.)

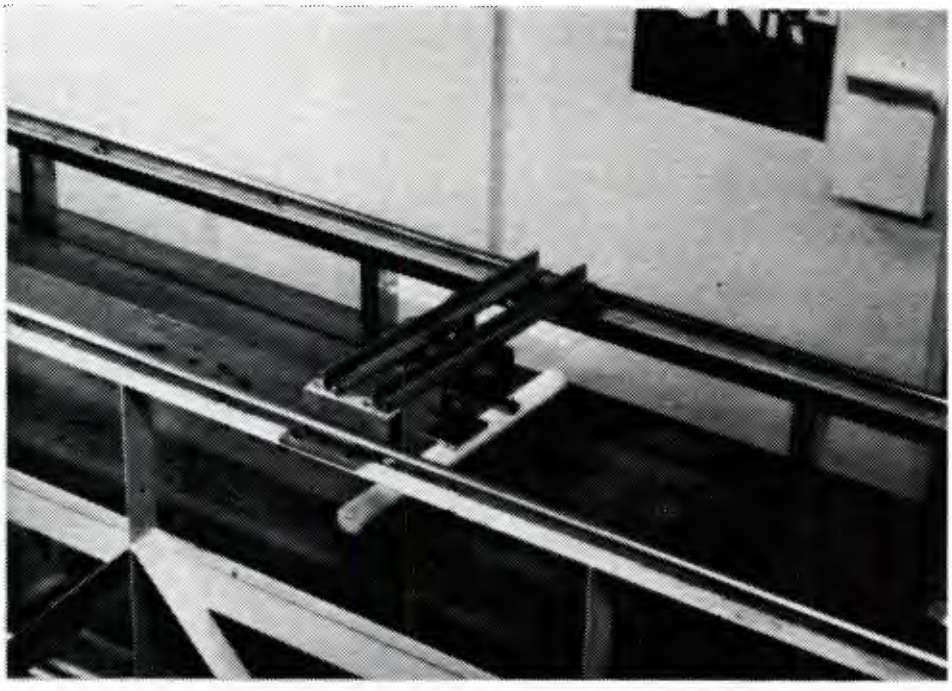

3a- Circular cylinder mounted in the flume.

3b- Looking down the flume in the direction of the flow.

FIGURE 3: Experimental set up.

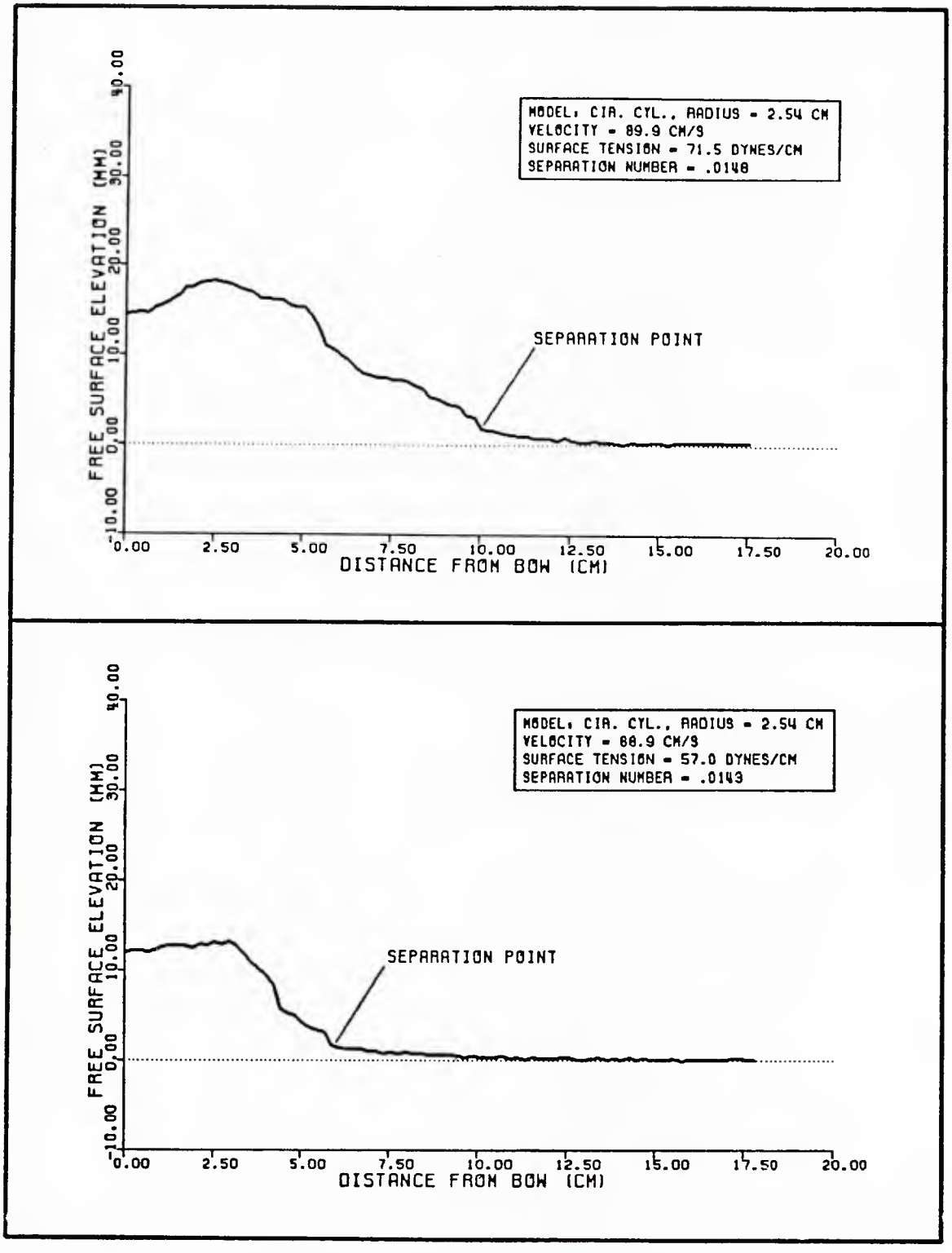

FIGURE 4: Example of an instantaneous wave profile used to measure the free surface slope at the separation point.

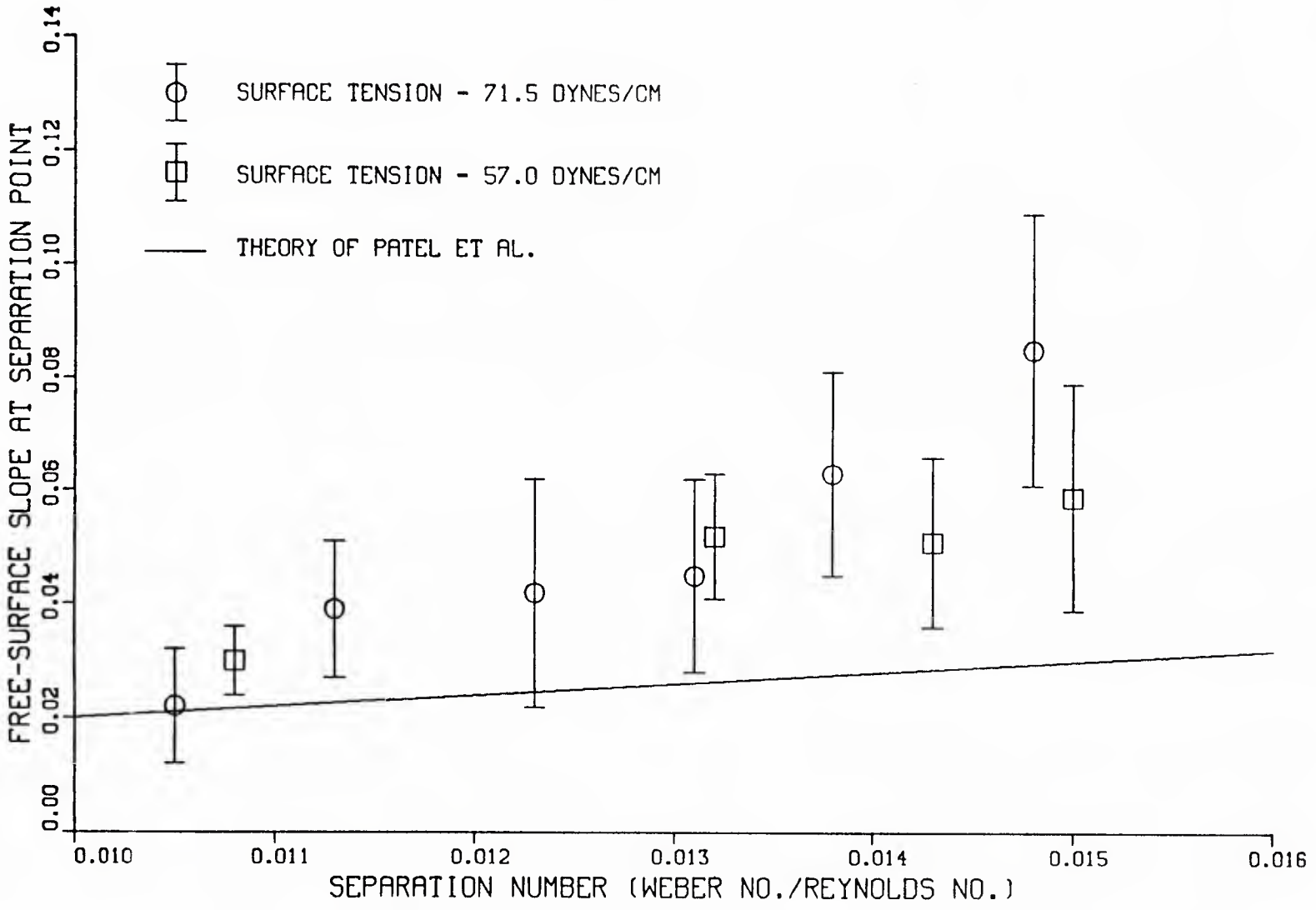

FIGURE 5: Free surface slope versus the separation number.

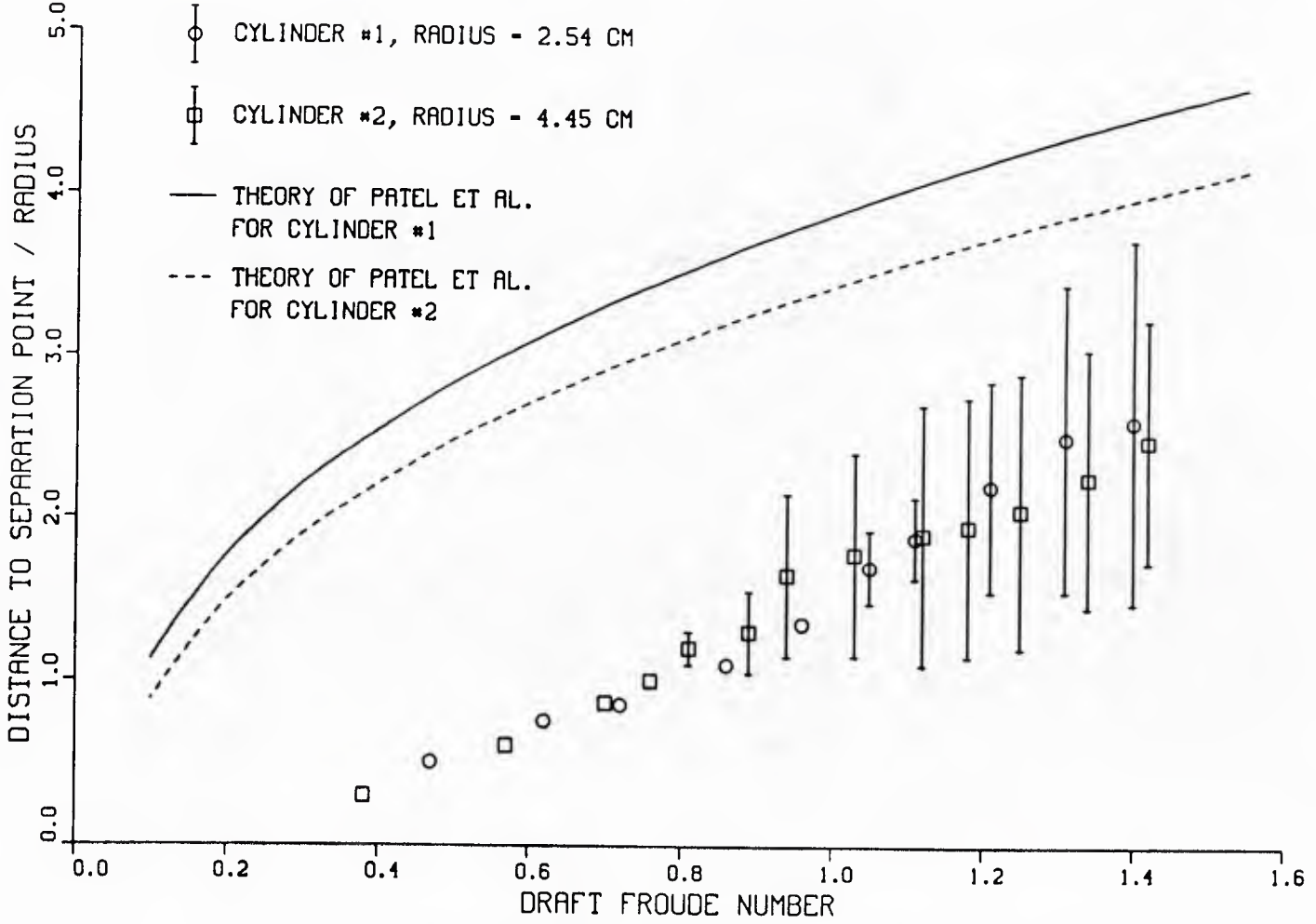

FIGURE 6: Nondimensionalized distance (distance/radius) to the separation point versus the draft Froude Number.

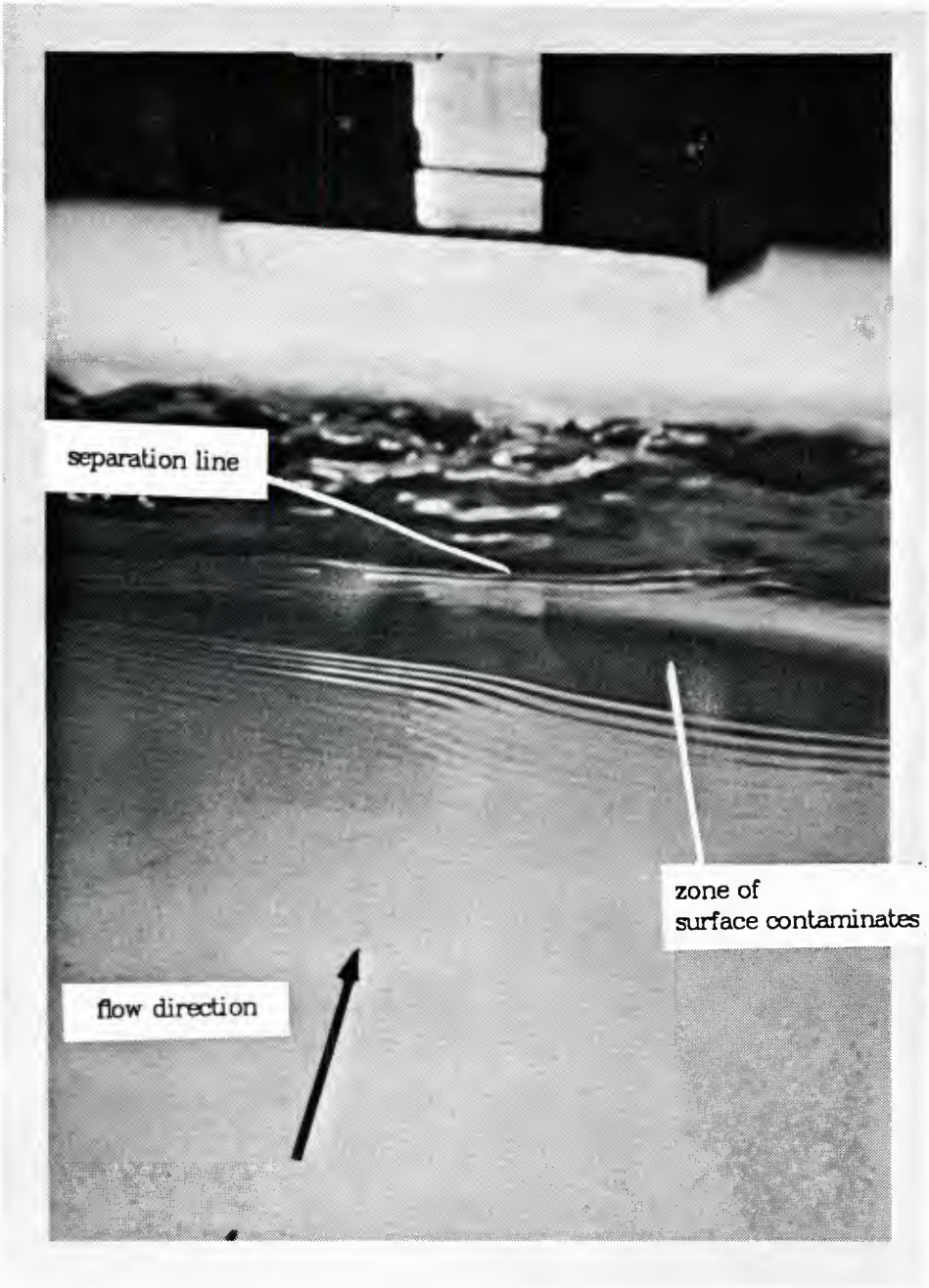

FIGURE 7: Surface contaminates collecting between the separation point and the capillary waves.

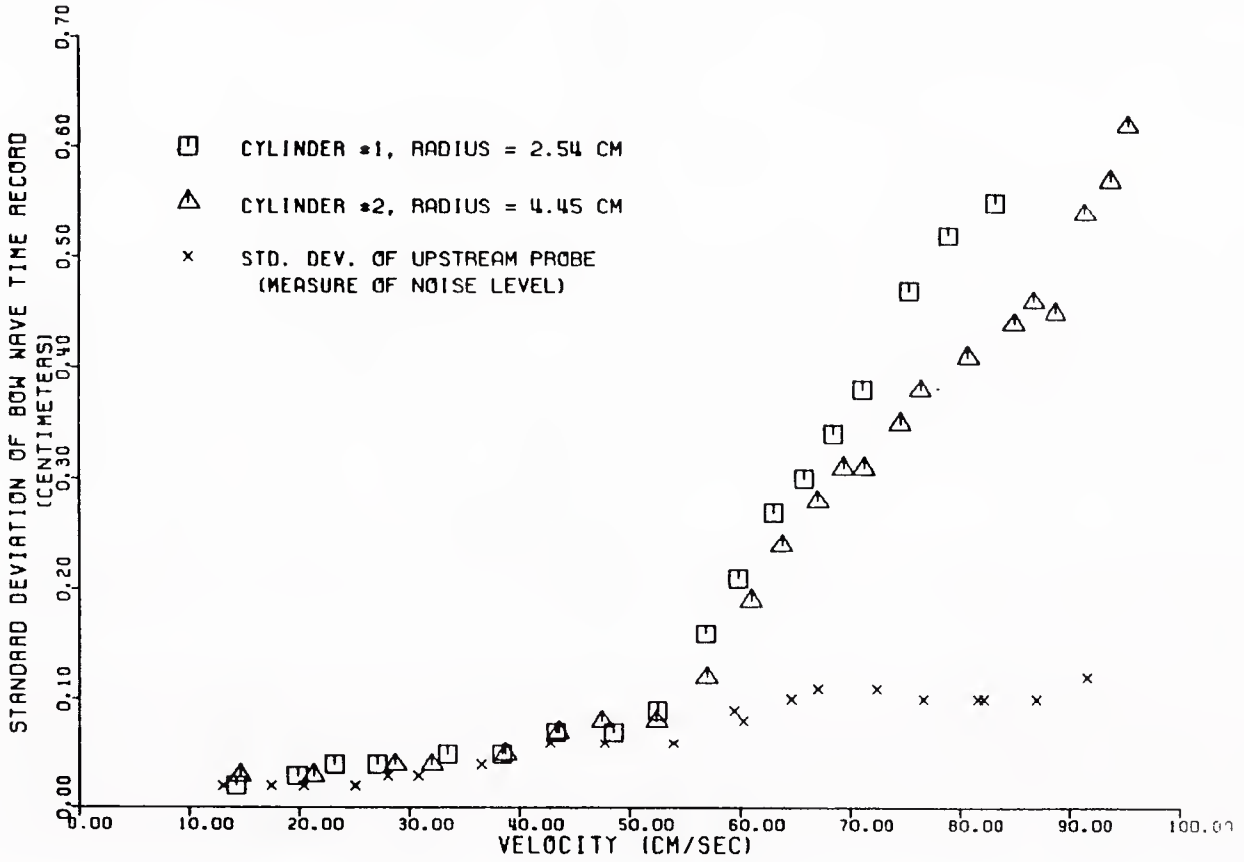

FIGURE 8: Standard deviations of bow wave time records for cylinder #1 and cylinder #2 plotted against the flow velocity. The x's are the standard deviations of time records of a probe that is mounted upstream of the bow wave region. They are a measure noise in the flume.

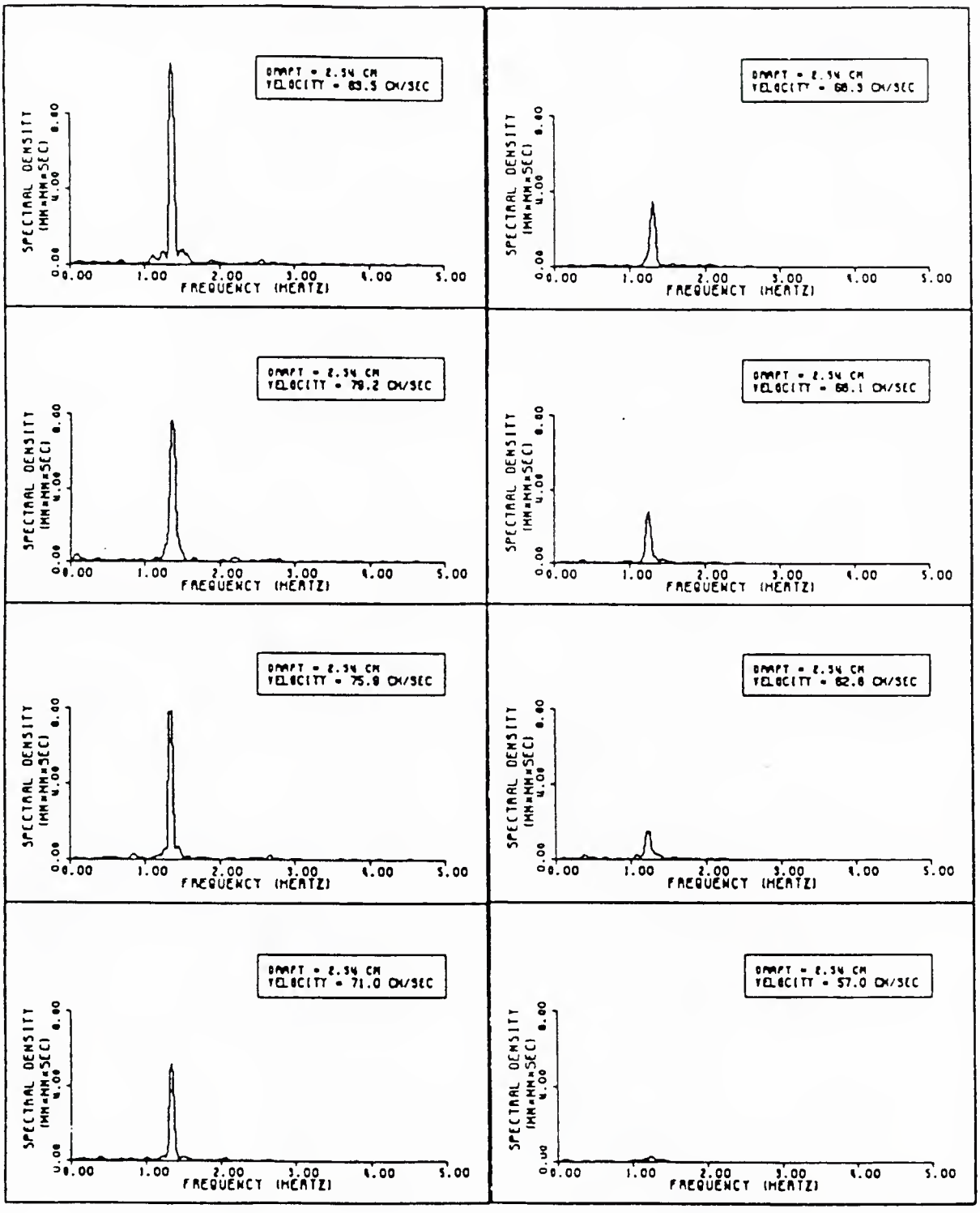

FIGURE 9: Power spectra of the bow wave time records for cylinder #1, radius = 2.54 cm. The ends are **unblocked**.

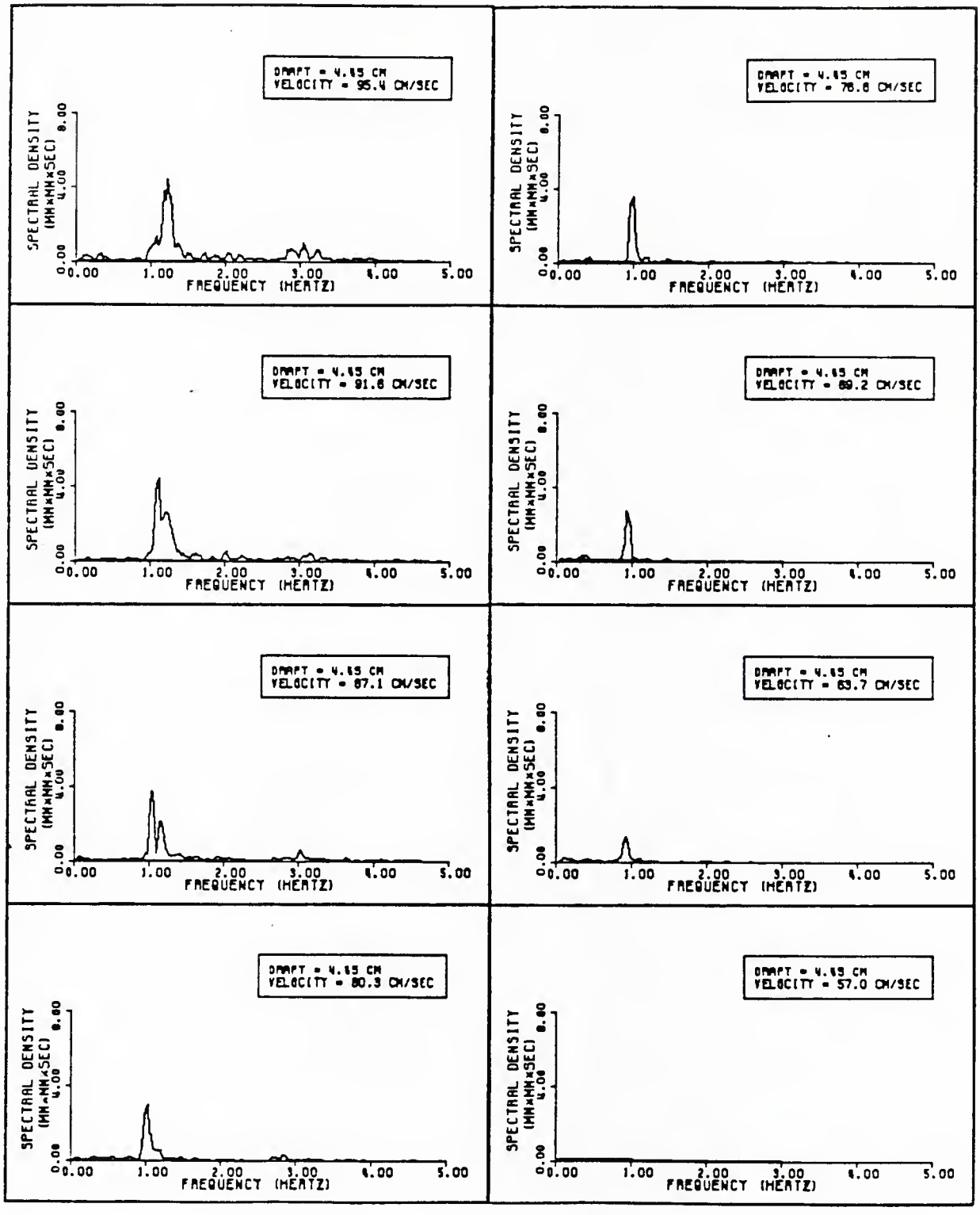

FIGURE 10: Power spectra of the bow wave time records for cylinder #2, radius = 4.45 cm. The ends are unblocked.

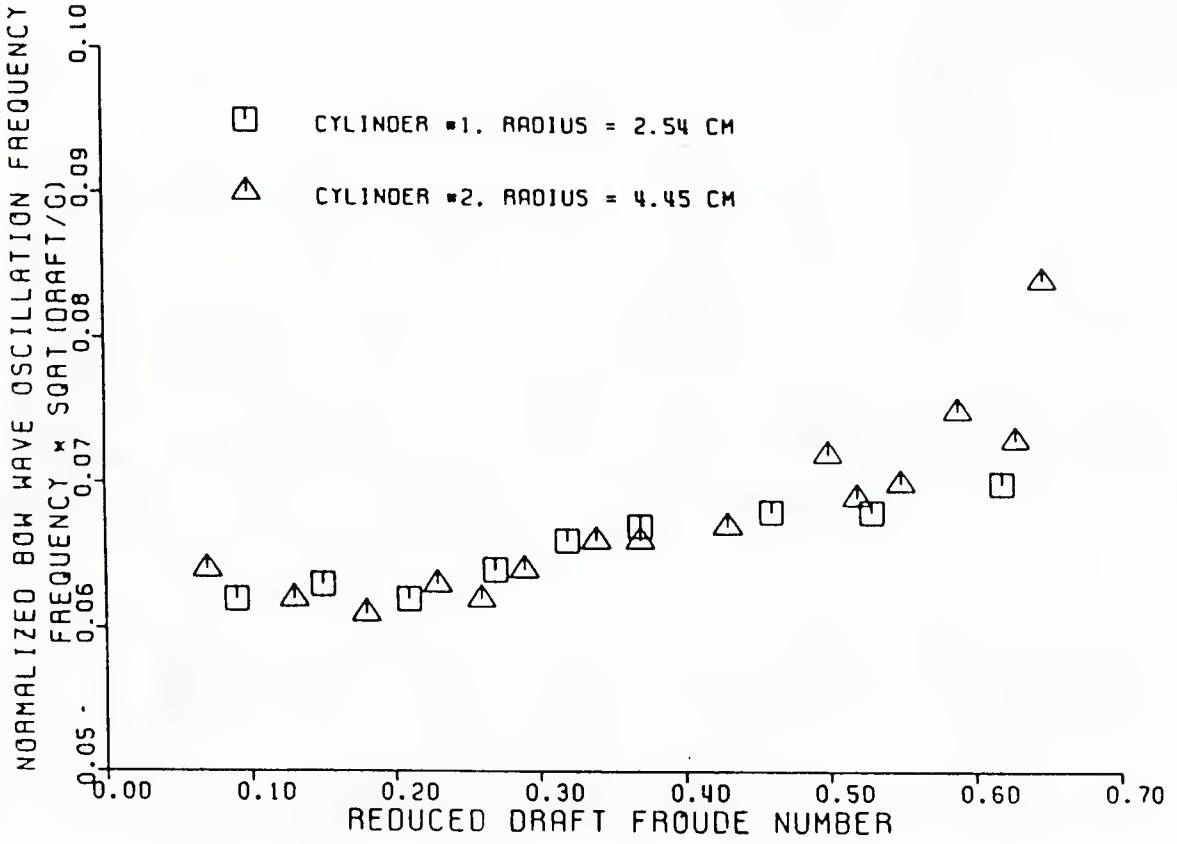

FIGURE 11: Frequency (nondimensionalized with the draft and gravitational acceleration) plotted against the reduced Froude Number.

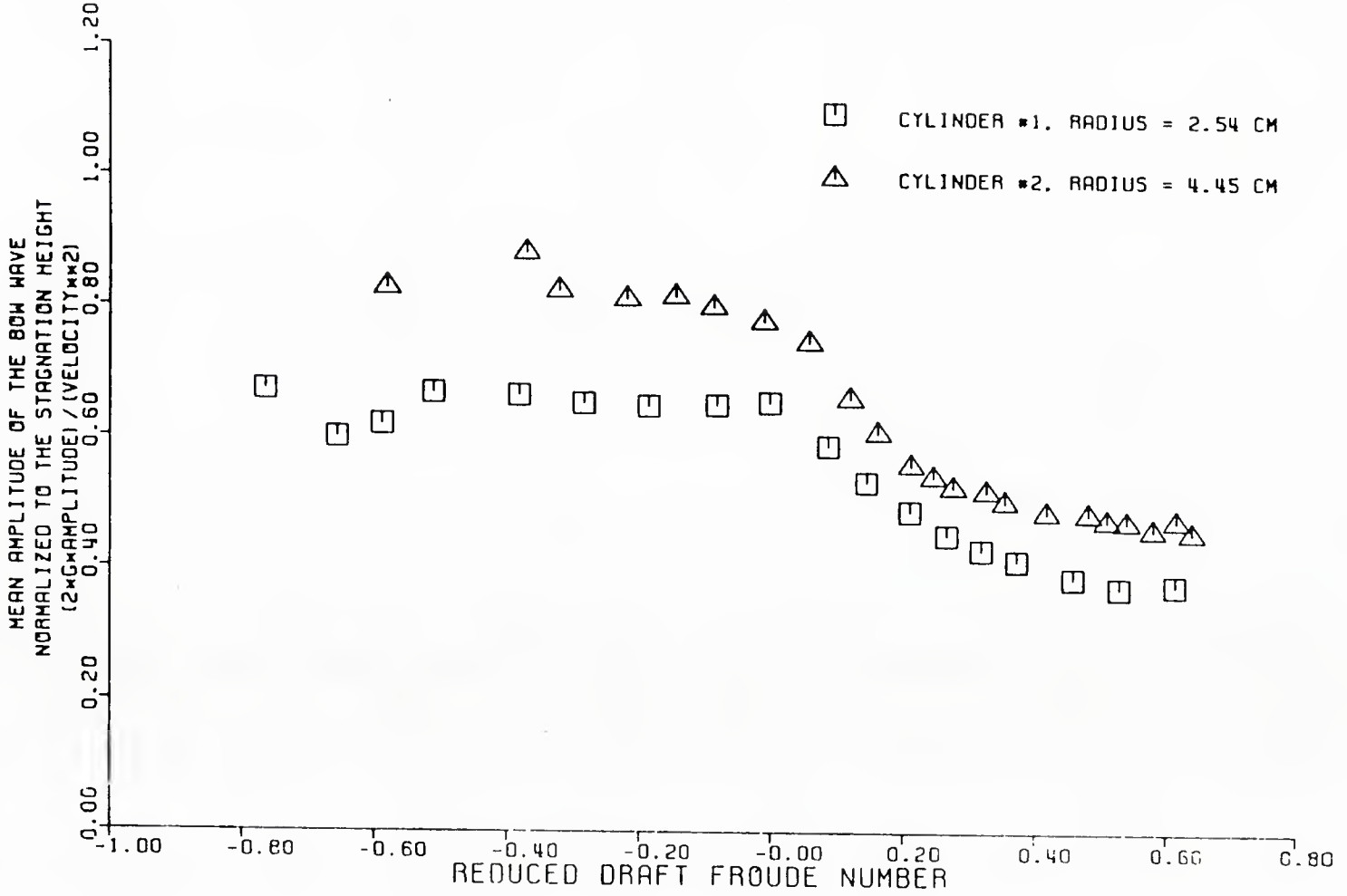

FIGURE 12: Mean amplitude of the bow wave time records (nondimensionalized by the total head of the incident stream) plotted versus the reduced Froude Number.

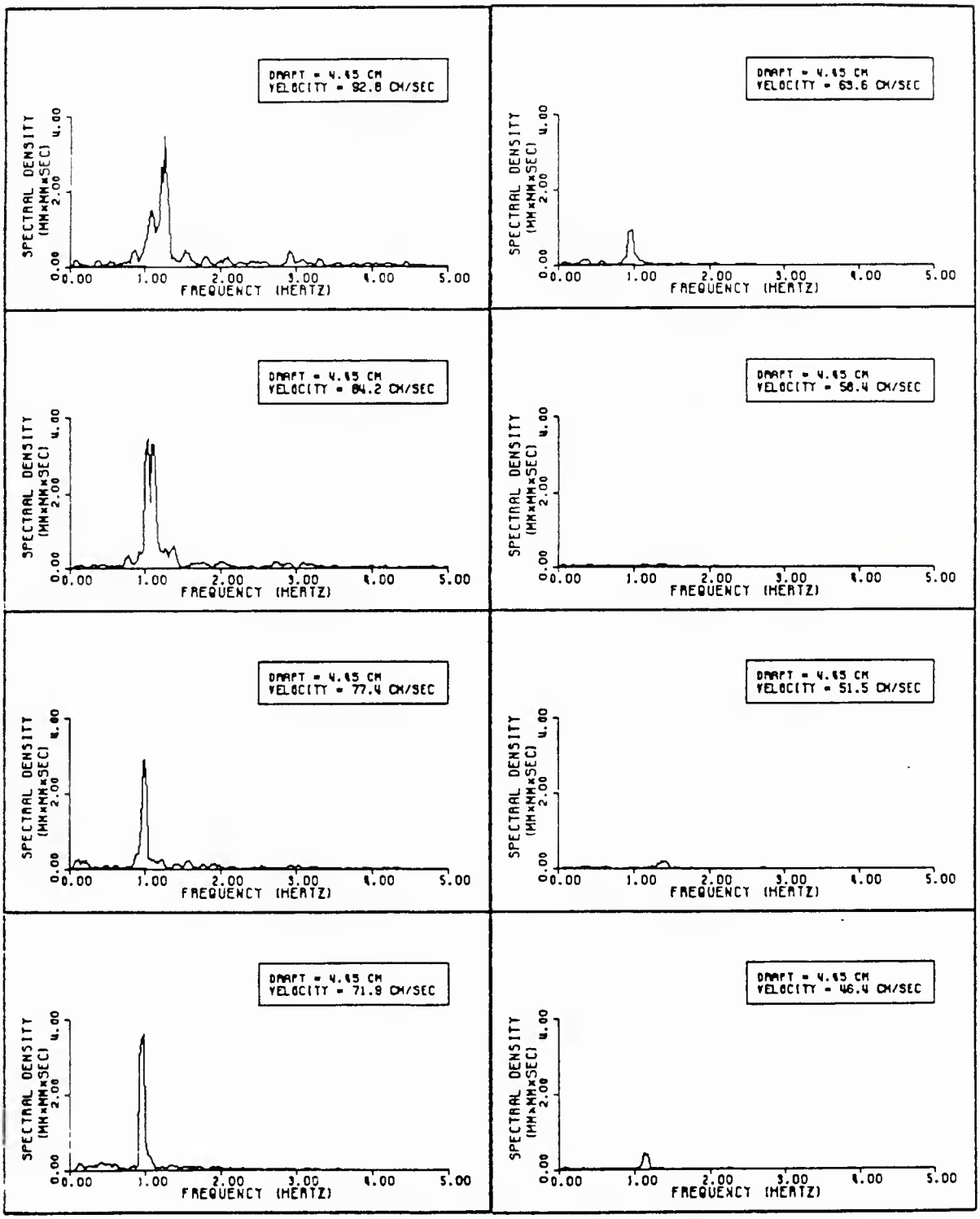

FIGURE 13: Power spectra of the bow wave time records for cylinder #2 with the ends blocked

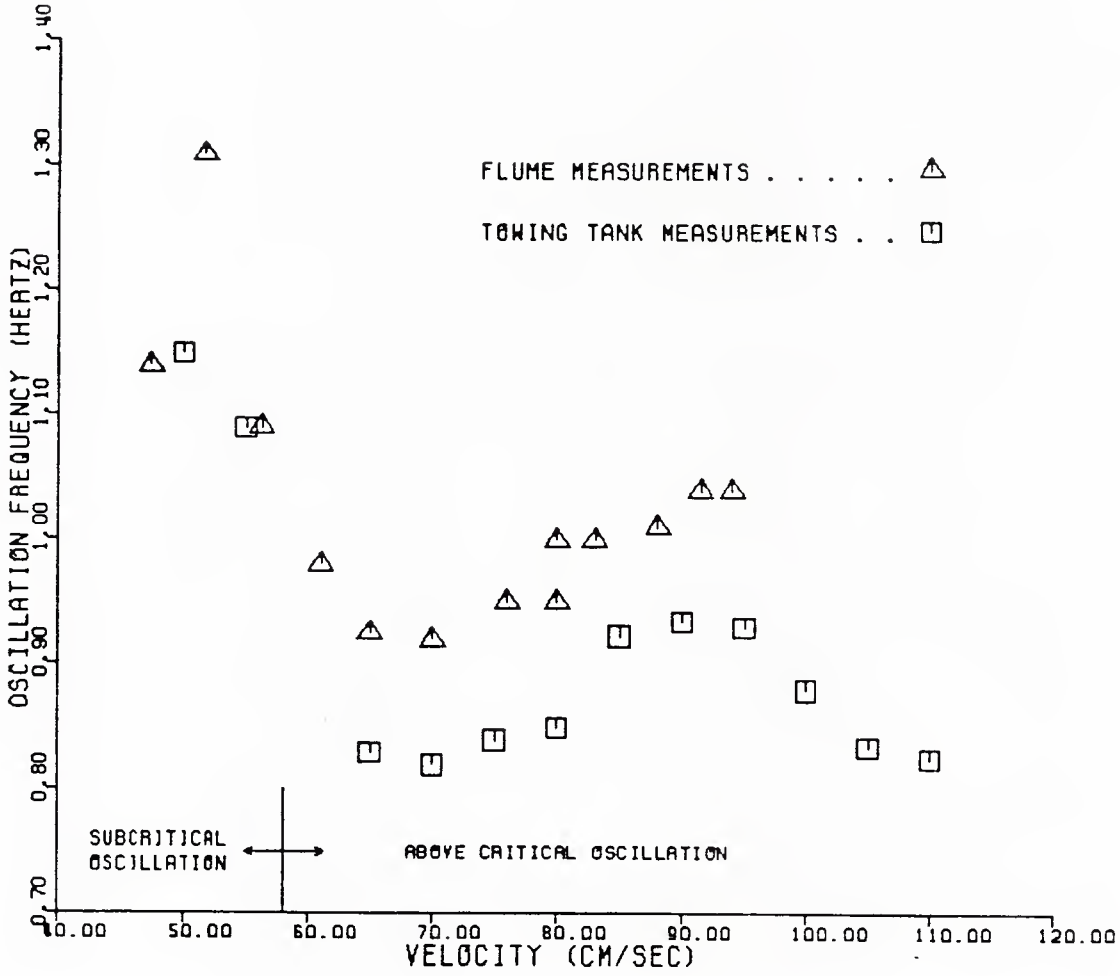

FIGURE 14: Frequency of oscillation versus velocity for cylinder #2. The triangles represent measurements made in the flume with the ends **blocked**. The squares represent measurements made in the towing tank. There, the flow was allowed to go around the ends. Note that the subcritical oscillation depends on the presence of surfactants.